Experimental Analysis and Modeling of Orthogonal Cutting Using Material and Friction Models

E. Ozlu, E. Budak

Faculty of Engineering and Natural Sciences, Sabanci University, Istanbul, Turkey

Abstract
In this study, a process model for orthogonal cutting processes is proposed. The model involves the primary and secondary deformation zones. The primary shear zone is modeled by a Johnson-Cook constitutive relationship and a shear plane having constant thickness. The secondary deformation zone is modeled semi-analytically, where the coefficient of friction is calibrated experimentally. The cutting forces predicted using the calibrated sliding friction coefficients are in good agreement with the measurements. The experimental investigation of sliding friction coefficients also show promising results for the proposed model, which is still under development.

Keywords:
Orthogonal Cutting, Friction, Process Model

1   INTRODUCTION

Being the fundamental model for all cutting processes, modeling of the orthogonal cutting has been one of the most important problems for machining researchers for decades. Understanding the true mechanics and dynamics of the orthogonal cutting process would result in solution of major problems in machining such as parameter selection, accurate predictions of forces, stresses, and temperature distributions. The first successful mathematical attempt for understanding of the mechanics of orthogonal cutting is made by Merchant [1]. Merchant [1] studied the continuous type chips and formulated the deformation zone, i.e. the shear plane, that is responsible for the formation of the chip by force equilibrium and the minimum energy principle. Although his work has several important assumptions, it is still widely used to understand the basics of the cutting process. Later, many researchers [2-7] worked on the modeling of the orthogonal cutting. After some deceleration in the research on cutting process mechanics due to the developments in CNC and CAD/CAM technologies, the process research regained some momentum in recent years. Many predictive models have been proposed by means of analytical, semi-analytical or completely numerical methods up to now. Semi-analytical models, where some of the values are identified from the cutting tests, usually yield high prediction accuracy, however they may not always provide insight about the process [8-10]. In addition, the cutting tests can be time consuming depending on the number of variables and their ranges. On the other hand, numerical models, such as FEM, [11-14] could provide much more detailed information about the process, such as temperature and pressure distribution on the rake face, however their accuracy is questionable and the solution times can be very long. Some analytical models may provide sufficient insight about the process and the solution times are usually very short. They can be grouped in some categories such as the slip-line models [15-19], and thin and thick shear zone models [20-23].

It can be deduced from the previous studies that there are several accurate models for the primary shear zone. There are also several studies where the friction in machining is investigated [24-30]. However, there are still issues in modeling the rake contact zone which involves the friction between the tool and the workpiece due to the complex nature of the chip-tool contact. The objective of this study is to propose an orthogonal cutting model that integrates the primary and secondary deformation zones' effects on the cutting process. In modeling of the primary shear zone the study of Dudzinski and Molinari [21] is used. The model uses a thermo-mechanical constitutive relationship which is transformed to a Johnson-Cook type material model in this study. The shear plane is modeled having a constant thickness. In their later model, Dudzinski and Molinari [21] modeled the friction on the rake face as a temperature dependent value. However, they just considered sliding contact conditions which may be valid for very high cutting speeds. In this study, the rake face contact is modeled by considering dual zones. The material which exists from the primary shear zone enters the rake contact with a high normal pressure that creates a sticking friction region between the tool and the material. After a short distance, the contact state changes to sliding friction due to the decreasing normal pressure which can be formulated by the Coulomb friction law. Orthogonal tube cutting tests and non-cutting friction tests are conducted in order to verify the model and discuss the results. The outputs of the proposed model are the cutting forces, the stress distributions on the rake face and the length of the sticking and sliding zones. Although the model is still under development, the final aim of the model is to develop a cutting process model which needs minimum amount of calibration tests. The friction and material constants can be obtained from orthogonal cutting tests. After the calibration, the model can be applied for all machining operations using the same tool and workpiece material.

The paper is organized as follows. The proposed mathematical formulation is derived in detail in the next section. In section 3 the experimental identification of the friction between the tool and the workpiece material is presented. In the last section the experimental results is presented and discussed.

2   THE ORTHOGONAL CUTTING PROCESS MODEL

In the proposed model two main deformation zones are taken into account: the primary shear zone also called as the shear plane and the secondary deformation zone also

called as the rake contact. It should be mentioned here that the model proposed by Dudzinski and Molinari [21] is used to model the primary shear zone. On the other hand, the secondary shear zone is modeled semi-analytically i.e. the behavior is modeled analytically but the friction coefficient is identified from the experiments. The models will be presented in the following sections in detail.

2.1 The Primary Shear Zone Model

As mentioned earlier the primary shear zone model is implemented to the current analysis from Dudzinski and Molinari [21]. The model will be presented here briefly for the integrity of the formulation and approach. Although they used a different thermo-mechanical constitutive relationship in their model, a Johnson-Cook (JC) constitutive relationship is used in the current analysis as follows:

$$\tau = \frac{1}{\sqrt{3}}\left[A + B\left(\frac{\gamma}{\sqrt{3}}\right)^n\right]\left[1 + m\ln\left(\frac{\dot{\gamma}}{\dot{\gamma}_0}\right)\right]\left[1 - \left(\frac{T - T_r}{T_m - T_r}\right)^v\right] \quad (1)$$

where γ is the shear strain, $\dot{\gamma}$ is the shear strain rate, $\dot{\gamma}_0$ is the reference shear strain rate, T is the absolute temperature, T_r is the reference temperature, T_m is the melting temperature, and A, B, n, m, and v are the material constants. The plastic deformation is assumed to take place only at the shear plane, and with plane strain conditions. Also the shear plane is modeled as a thin plane but having a thickness of 0.025 mm. Moreover, the shear stress distribution at the outer boundary of the shear plane is assumed to be uniform. With the assistance of the equations of conversation of momentum and energy, and the constitutive law, Dudzinski and Molinari [21] proposed to solve a compatibility condition with an iterative procedure in order to calculate the shear stress at the entry of the shear plane, τ_0. Moreover again from the equations of motion for a steady state solution and continuous type chip The shear stress at the exit of the shear plane is calculated as follows [21,22]:

$$\tau_1 = \rho(V\sin\phi)^2\gamma_1 + \tau_0 \quad (2)$$

where ρ is the density of the material, V is the cutting speed, ϕ is the shear angle, and γ_1 is the shear strain at the exit of the shear plane. The shear angle in the model is calculated by the Merchant model as follows [1,22]:

$$\phi = (\pi/2 + \alpha - \lambda)/2 \quad (3)$$

where α is the rake angle, and λ is the mean friction angle which equals to atan(μ_a). However it should mentioned that the model proposed in this study uses the shear angles obtained from orthogonal cutting tests.

2.2 The Dual Zone Rake Face Contact Model

In this section the reasoning and the formulation for the dual zone rake face contact model is given, and an iterative solution procedure is proposed. The model proposed in this study divides the rake face into two regions as for the first time proposed by Zorev [3]. In the first region the contact condition is defined to be sticking due to the high normal pressure exerted on the tool, whereas in the second region the contact is considered to be the Coulomb (sliding) friction. Zorev [3] and some other later studies [31-33] define the shear stress and the normal stress distribution on the rake face as shown in Fig. 1.a. However it is well known and also proved by friction tests [34] that the Coulomb friction coefficient cannot exceed 1.0 between metallic materials unless some kind of oxide formation or chemical reaction occurs [26,35]. Therefore, as shown by split tool cutting tests and mathematical

analysis [18,28,34,36-38] the distribution of the shear and normal stress on the rake face is obtained as in Fig. 1.b. This distribution is used for the model in this study.
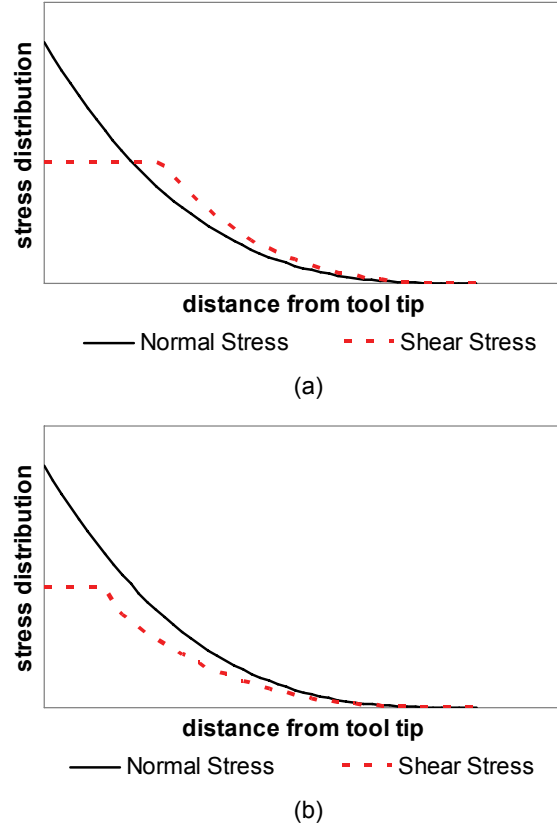

(a)

(b)

Figure 1: Stress distributions on the rake face by two different approaches, where the sliding friction coefficient is (a) higher, and (b) smaller than 1.

From Fig. 1.b, it can be observed that the shear stress on the rake is equal to the shear yield stress of the material (τ_1) along the sticking region with length ℓ_p. It should be noted here that in the thin shear plane model used in the analysis, the plastic deformation is assumed to occur only in the shear plane. Therefore τ_1 is equal to the shear stress at the exit of the shear band at the shear plane which is calculated by Eqn. (2). In addition, the shear stress in the sliding region is equal to the product of sliding friction coefficient (μ) and the normal stress (P), according to the Coulomb friction law. The shear stress reduces to zero at the end of the contact zone. Therefore, the mathematical representation of the shear stress distribution on the rake face can be defined as follows:

$$\begin{aligned}\tau &= \tau_1 & x \le \ell_p \\ \tau &= \mu P & \ell_p \le x \le \ell_c\end{aligned} \quad (4)$$

where ℓ_c is the contact length, and x is the distance on the rake face from the tool tip. Moreover the shear stress distribution along the sliding friction region can be defined as follows:

$$\tau(x) = \tau_1\left(1 - \frac{x - \ell_p}{\ell_e}\right)^\zeta \quad \ell_p \le x \le \ell_c \quad (5)$$

where ℓ_e is the length of the sliding region. Also for the normal stress on the rake face the following distribution, which is validated by various researchers and experiments for metallic materials [22, 28, 36], is selected:

$$P(x) = P_0\left(1 - \frac{x}{\ell_c}\right)^\zeta \tag{6}$$

where P_0 is the normal stress on the rake face at the tool tip, and can be found as follows: The normal force acting on the rake face can be obtained as (see Fig. 2):

$$N = \int_0^{\ell_c} P(x) = \int_0^{\ell_c} P_0\left(1 - \frac{x}{\ell_c}\right)^\zeta w dx = P_0\frac{w\ell_c}{\zeta + 1} \tag{7}$$

where w is the width of cut. The normal force N can also be calculated in terms of the shear force on the shear plane is:

$$N = F_s\frac{\cos\lambda}{\cos(\phi + \lambda - \alpha)} \tag{8}$$

where the shear force F_s is defined as follows by assuming that the shear stress distribution on the shear plane AB is uniform:

$$F_s = \tau_1\frac{wh_1}{\sin\phi} \tag{9}$$

where h_1 is the uncut chip thickness. Combining Eqns. (7-9) P_0 can be calculated as follows [22]:

$$P_0 = \tau_1\frac{h_1(\zeta + 1)}{\ell_c\sin\phi}\frac{\cos\lambda}{\cos(\phi + \lambda - \alpha)} \tag{10}$$
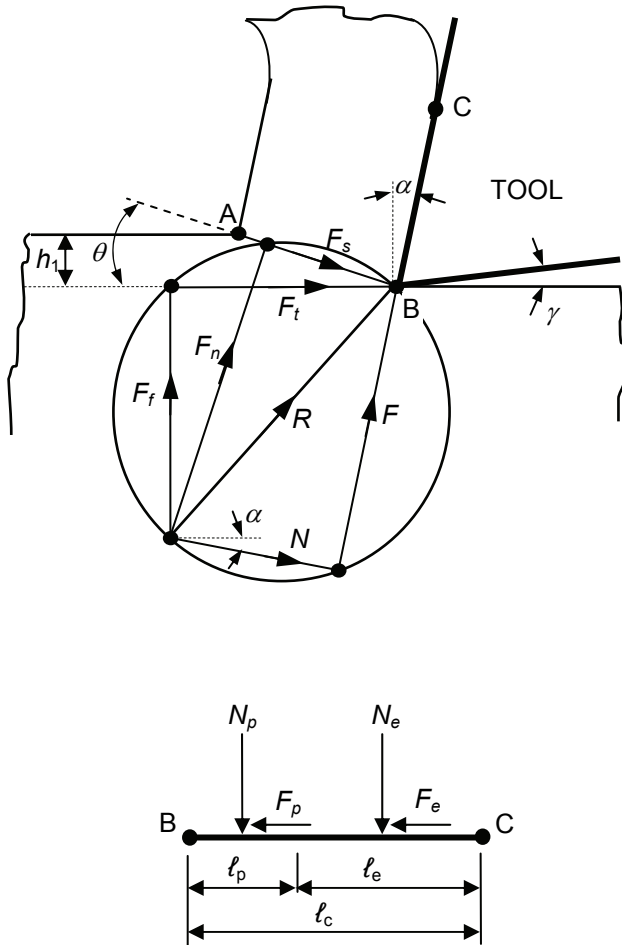

Figure 2: The Merchant's Circle and the schematic representation of the forces acting on the rake face.

The next step is to calculate the length of contact ℓ_c. Assuming that the normal stress is distributed uniformly at the exit of the shear plane, and considering the momentum equilibrium at the tool tip, we get: $M_{AB} = M_{BC}$

$$M_{AB} = F_n\frac{AB}{2} = F_s h_1\frac{\tan(\phi + \lambda - \alpha)}{2\sin\phi} \tag{15}$$

$$M_{BC} = \int_0^{\ell_c} xP_0\left(1 - \frac{x}{\ell_c}\right)^\zeta w dx = F_s\frac{\ell_c}{\zeta + 2}\frac{\cos\lambda}{\cos(\phi + \lambda - \alpha)} \tag{16}$$

From Eqns. (15) and (16), the contact length ℓ_c is obtained as follows [28]:

$$\ell_c = h_1\frac{\zeta + 2}{2}\frac{\sin(\phi + \lambda - \alpha)}{\sin\phi\cos\lambda} \tag{17}$$

Now we can be able to calculate the length of the sticking region ℓ_p. For the sliding region we have that (see Fig. 2):

$$F_e = \mu N_e \tag{18}$$

The normal N_e and friction forces F_e can be calculated as follows:

$$N_e = \int_{\ell_p}^{\ell_c} P_0\left(1 - \frac{x}{\ell_c}\right)^\zeta w dx = P_0\frac{w\ell_e}{\zeta + 1}\left(\frac{\ell_p}{\ell_c} - 1\right)^{\zeta + 1} \tag{19}$$

$$F_e = \int_{\ell_p}^{\ell_c} \tau_1\left(1 - \frac{x - \ell_p}{\ell_e}\right)^\zeta w dx = \tau_1\frac{w\ell_e}{\zeta + 1} \tag{20}$$

Substituting Eqns. (19) and (20) into Eqn. (18) and expanding $\ell_e = \ell_c - \ell_p$ we obtain the length of the sticking region as follows:

$$\ell_p = \ell_c\left(\left(\pm\frac{\tau_1}{P_0\mu}\right)^{1/\zeta} + 1\right) \tag{21}$$

The term inside the root is positive if ζ is an even number, and it is negative if ζ is odd number. The only parameter left to be defined is the apparent friction coefficient, μ_a. The apparent friction coefficient is defined as follows:

$$\mu_a = F/N \tag{22}$$

The normal force acting on the rake face N can be obtained from Eqn. 11 and the friction force on the rake face F can be calculated as follows:

$$F = \int_0^{\ell_p} \tau_1 w dx + \int_{\ell_p}^{\ell_c} \tau_1\left(1 - \frac{x - \ell_p}{\ell_e}\right) w dx = \tau_1 w\left(\ell_p + \frac{\ell_e}{\zeta + 1}\right) \tag{23}$$

Substituting Eqn. (11) and (23) into Eqn. (22), μ_a is obtained as follows:

$$\mu_a = \frac{\tau_1}{P_0}\frac{\ell_p(\zeta + 1) + \ell_e}{\ell_c} \tag{24}$$

2.3   The Solution Procedure for Cutting Forces

In this section the application of the derived formulation to the orthogonal cutting process will be discussed. Basically two scenarios are considered in this study. Firstly, the input parameters for the model are summarized in Table 1. As can be seen from Table 1 only the apparent and the sliding

friction coefficients are unknown. As the first case the sliding coefficient of friction can be identified from non-cutting friction tests whereas in the second case, the apparent friction coefficient can be obtained from orthogonal tube cutting tests. The details of these experiments are discussed in Section 3. Although the approach is the same, two different solution procedures are proposed for these two different cases, which can be seen in Fig. 3 a. and b. simultaneously.

In the first case where the sliding friction coefficient is known, the iterative procedure starts with a small value of the apparent friction coefficient, e.g. 0.1. Then, the necessary calculations are done as shown in Fig. 3.a in detail. At the end of the iteration an apparent friction coefficient is obtained as derived in Eqn. (24). If the difference between the calculated μ_a and the initially guessed one is in the desirable range the iteration procedure stops, else continues by increasing the initial μ_a value. In the second case where the apparent friction coefficient is known, a similar iterative procedure is applied in order to solve for sliding friction coefficient as shown in Fig. 3.b in detail. After the iteration converges in both cases, the cutting forces can be calculated as follows:

$$F_t = \tau_1 \frac{wh_1}{\sin\phi} \frac{\cos(\lambda - \alpha)}{\cos(\phi + \lambda - \alpha)}$$
$$F_f = \tau_1 \frac{wh_1}{\sin\phi} \frac{\sin(\lambda - \alpha)}{\cos(\phi + \lambda - \alpha)}$$

(25)

where F_t is the tangential force at the cutting velocity direction and F_f is the feed force at the feed (thrust) direction (see Fig. 2).

Table 1: Parameters needed for the cutting force analysis.

Parameters	Explanation
Depth of cut	Process dependent
Feed rate	Process dependent
Rake angle	Process dependent
Pressure distribution – ζ	Selected as 3
Workpiece diameter	Process dependent
Spindle speed	Process dependent
Material constants	From experiments
Fraction of energy converted to heat at the shear plane	From empirical values, selected as 0.95 [39]
Thickness of the primary shear zone	Selected as 0.025 mm [21]
Sliding friction coefficient	Unknown
Apparent friction coefficient	Unknown

It should be noted here that our ultimate aim in these simulations is to calibrate the sliding friction coefficient between the tool and the workpiece material. The calibration involves the identification of apparent friction coefficient from orthogonal tube cutting tests, and using the method described in Fig. 3.b, the sliding friction coefficient is calibrated for different feed rates and cutting speeds, also indirectly the average pressure exerted on the rake face. The difference of this methodology from classical orthogonal cutting tests is that these set of tests do not depend on the rake angle. Thus, the tests can be carried out by one tool only, i.e. one rake angle. The model will handle the cases for different rake angles, once the calibrated sliding friction coefficient is used to predict the forces with the method described above and in Fig. 3.a.

3 IDENTIFICATION OF FRICTION COEFFICIENT BETWEEN THE TOOL AND THE WORKPIECE

In this section two different experimental methods are described in order to identify the friction coefficient between the tool and the workpiece material which would complete the proposed process model. In the first method, non-cutting tests, the friction coefficient μ due to the sliding contact between the tool and workpiece materials is measured. On the contrary in the latter method the aim is to identify the apparent friction coefficient on the rake face where an orthogonal database is obtained by tube cutting tests. The experimental results together with the process model results are discussed in Section 4.
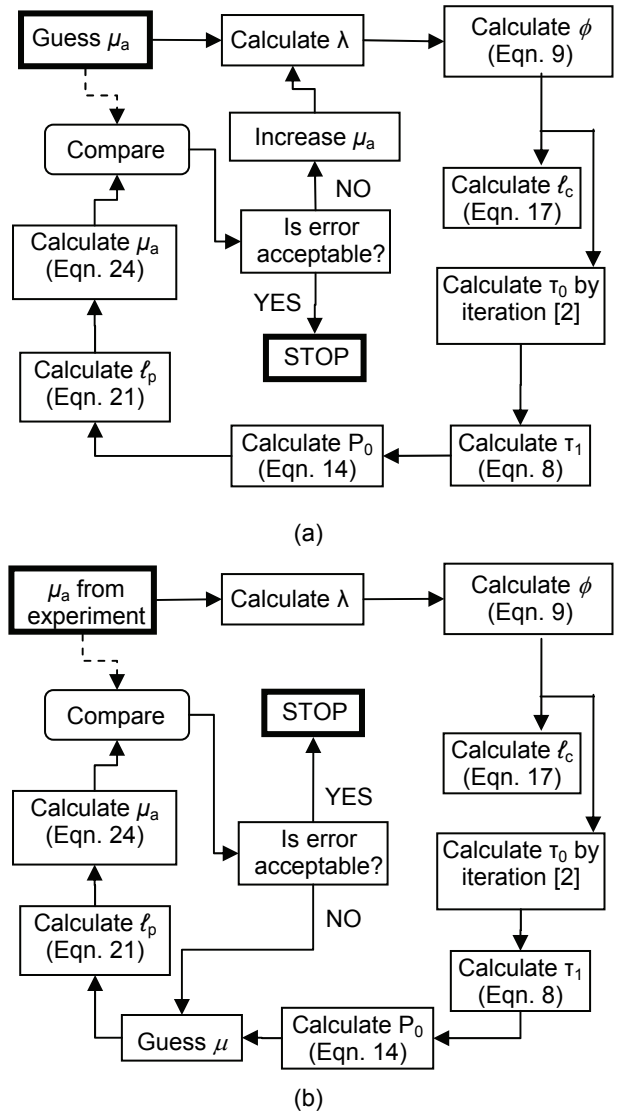

(a)

(b)

Figure 3: Solution procedure when (a) sliding coefficient of friction is known, or when (b) apparent friction coefficient is known.

3.1 Friction Coefficients from Non-Cutting Tests

In order to obtain the sliding coefficient of friction between the workpiece and the cutting tool materials a non-cutting friction test setup is prepared. The setup is built on a manual lathe. As can be seen in Fig. 4, the setup involves a dynamometer in order to measure the normal and the friction forces, a fine slider in order to make the initial contact between tool and workpiece smoother, and a DAQ

setup in order to collect the data. It should be noted that an uncoated carbide rod is used in the experiments to as the tool material and the workpiece material was AISI 1050 steel. The 3 mm diameter carbide rods were present which were placed at the origin axis of the workpiece in order to avoid the third force (i.e. the radial force) component. The sliding friction speed is controlled by moving the carbide rod along the radial axis of the workpiece. The sliding coefficient of friction is calculated using the mean values as shown in Fig. 5 for an example case:

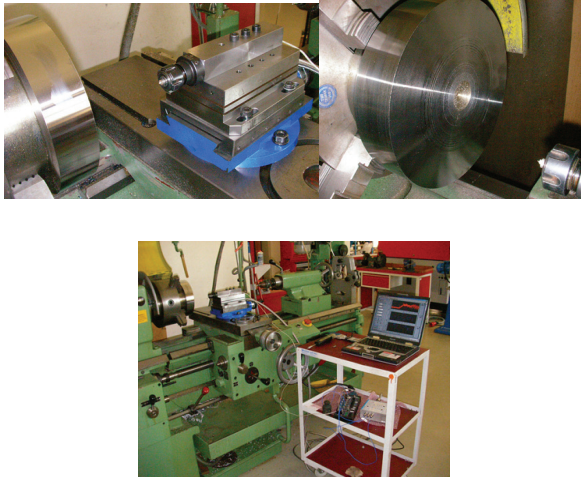$$\mu = F_{friction} / F_{normal} \qquad (26)$$

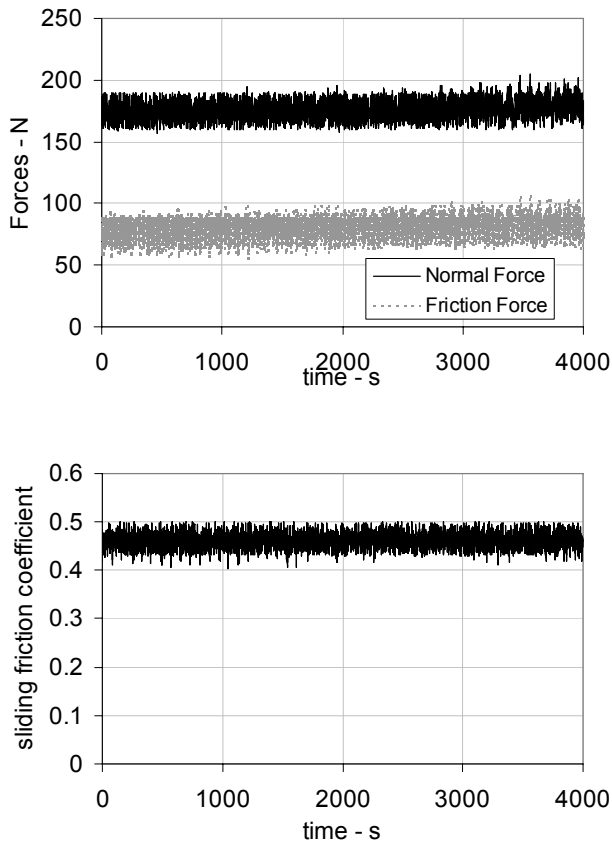

Figure 4: The non-cutting test setup.

Figure 5: An example case of calculating the mean Coulomb friction coefficient by measured force data at 420 m/min friction speed.

It should be mentioned that the non-cutting friction tests are done in order to verify the proposed model. They do not have any contribution to the force prediction procedure

that is discussed in Section 2. Only the apparent friction coefficient is needed as the sliding friction coefficient for different feed rates and cutting speeds are calibrated.

3.2 Friction Coefficients from Orthogonal Tube Cutting Tests

In order to measure the apparent coefficient of friction on the rake face, we conducted orthogonal tube cutting tests on a conventional lathe. The test setup involves a dynamometer and a DAQ setup in order to collect the cutting force data. After each experiment the cut chip thickness is measured by two methods and the mean value of the cut chip thickness is used for shear angle calculations. In the first measurement method, the cut chip thickness is simply measured by a micrometer. In the second method the average thickness of the cut chip is determined from weight measurements.

The workpiece material was AISI 1050 steel and 4 types of inserts were used in the tests: coated and uncoated carbide, ceramic and CBN inserts. The inserts were of TPGN type i.e. the rake face of the insert is flat with 5º rake angle. All the tests were conducted at dry condition except one case. The tests were conducted at different cutting speeds and feed rates. The cutting speed range was 150 – 1200 m/min and the feed rate range was 0.05-0.16 mm/rev. The apparent friction coefficient on the rake face between the tool and the workpiece is calculated as follows:

$$\mu = \tan\left(rake + a\tan\left(F_f / F_t\right)\right) \qquad (27)$$

where F_f and F_t are the measured feed and tangential forces, respectively. The results are discussed in the following section.

4 RESULTS AND DISCUSSION

The results obtained from the non-cutting and orthogonal cutting tests are presented in this section together with the force predictions of the proposed process model, and comparison with the experimental results.

4.1 Coefficient of Friction Measurements

The results obtained from the non-cutting and the orthogonal tube cutting tests are discussed in this section. The apparent friction coefficients measured at different cutting speeds and feed rates for different insert types can be found in Fig. 6. As can be observed from the results, there is a slight decrease in friction coefficient with the cutting speed and the feed rate for each insert. The maximum apparent friction coefficient is measured to be around 0.6 which corresponds to the coated carbide inserts. The minimum friction coefficient is measured to be around 0.3 for CBN with dry cutting conditions and uncoated carbide insert with coolant. Another important conclusion is derived when the sliding coefficient of friction values are compared with the apparent coefficient of friction values for uncoated carbide tools (see Fig. 7). As expected, the apparent friction coefficients are found to be slightly smaller than the sliding coefficients of friction. This is due to the existence of the sticking region.

Another conclusion which can be deduced from Fig. 7 is that the sliding friction coefficient between the uncoated carbide tool and AISI 1050 steel doesn't depend on the friction speed strongly. However, there is a slight decrease in the sliding coefficient of friction at moderate speeds.

● CBN   ■ CERAMIC
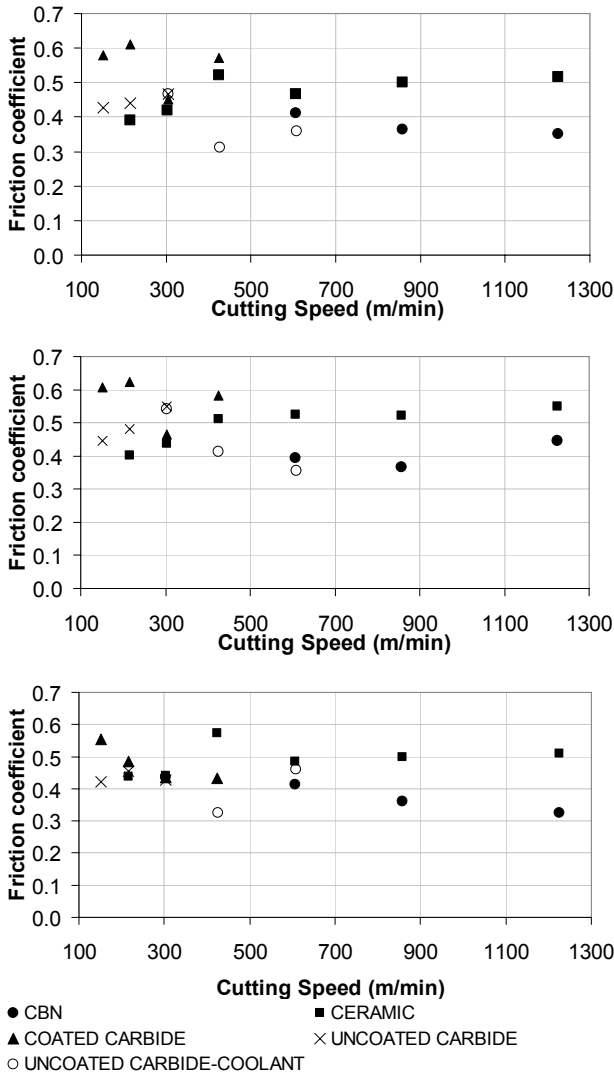▲ COATED CARBIDE   ✕ UNCOATED CARBIDE
○ UNCOATED CARBIDE-COOLANT

Figure 6: Apparent friction coefficients obtained from orthogonal cutting tests for different cutting speeds, and type of inserts for feed rates of (a) 0.05, (b) 0.08, and (c) 0.16 mm/rev.
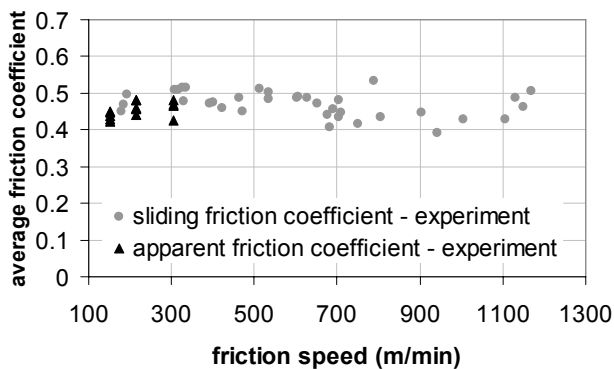

Figure 7: Sliding coefficient of friction obtained from non-cutting tests together with the apparent friction coefficient.

4.2 An Example Case for the Process Model

In this section an example single case is presented in order to demonstrate the proposed model predictions. The parameters used in the analysis can be found in Table 2.

Table 2: The parameters that are used in the example case.

Depth of cut	1 mm	**Material Constants**	
Feed rate	0.08 mm/rev	A	850 MPa
Rake angle	5º	B	600 MPa
Pressure dist. – ζ	3	C	0.02
Workpiece dia.	30 mm	N	0.165
Spindle speed	3000 rpm	M	1
Sliding fric. coeff.	0.6	$\dot{\gamma}$	0.01

The resulting stress distribution can be found in Fig. 8. As also can be observed from Fig. 8 the contact length is calculated as 0.35 mm and the sticking region length is calculated as 0.06 mm. In addition, F_t is calculated as 182 N and F_f is calculated as 92 N, and the apparent coefficient of friction is calculated as 0.5.
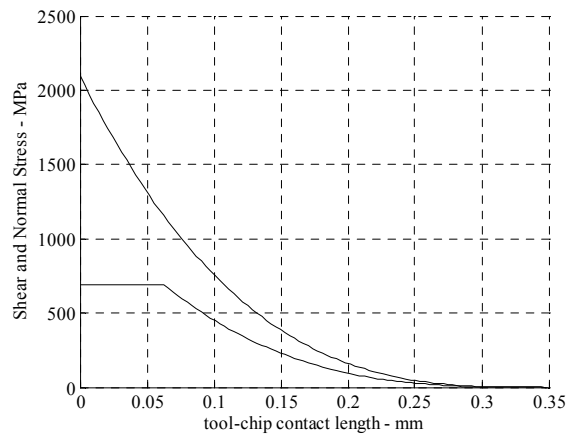

Figure 8: The stress distributions on the rake face for the example case.

4.3 Identification of Sliding Coefficient of Friction from the Process Model

In this section, the proposed model is verified in terms of the friction coefficient calculations. The apparent coefficient of friction values obtained from the orthogonal tube cutting tests are used as input to the model, and the sliding coefficients of friction are calculated. The material constants for the JC constitutive model used in the analysis for AISI 1050 steel are listed in Table 2. The calculated sliding coefficients of friction for the uncoated carbide tool for different cuttings speeds and average pressure on the sliding region can be found in Fig. 9.
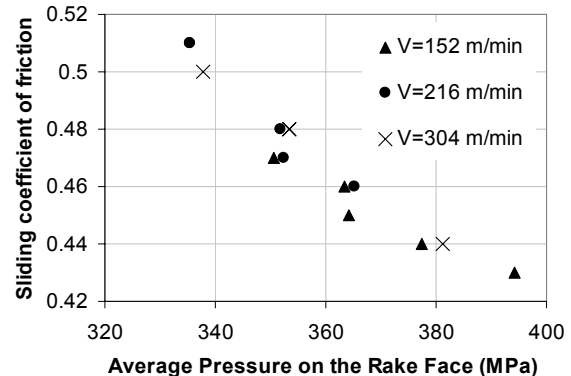

Figure 9: The sliding coefficient of friction calculated from the process model for uncoated carbide tool and variation for average pressure exerted on the rake face.

Also the experimental apparent and sliding friction coefficient results along with the sliding friction coefficient calculated from the process model can be found in Fig. 10.
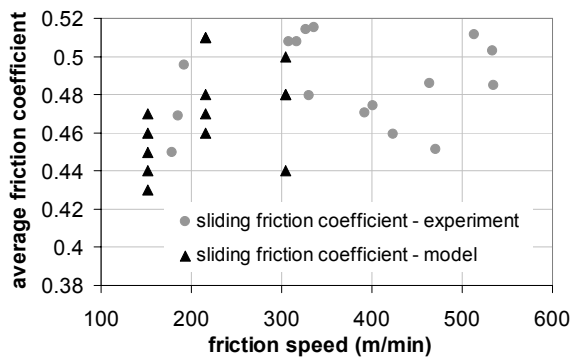

Figure 10: The experimentally identified sliding coefficient of friction and the process model results.

As can be seen from Fig. 9 the sliding coefficient of friction decreases with the increasing pressure as expected. And also from Fig. 10 it can be seen that the experimental measurements and the results obtained from the model is in close agreement.

4.4 Comparison of Force Predictions with the Experimental Results

In this section, the proposed process model is compared with the experimental results in terms of force predictions. Again the material constants used in the analysis for AISI 1050 steel is selected as listed in Table 2. The apparent coefficient of friction obtained from the orthogonal cutting tests are used as an input to the model and the tangential and feed cutting forces are calculated by the proposed model and compared with the forces obtained from the same tests. The results can be seen in Fig. 11 for different cutting speeds and feed rates. Good agreement is observed between the predictions and the measurements.

5 CONCLUSIONS

The process model proposed in this paper for orthogonal cutting operations takes the primary and secondary deformation zones into account. The primary shear zone modeling is adapted from Dudzinski and Molinari [21] and the contact on the rake face is modeled by a dual zone model. The rake face contact is divided into two regions where in the first region the contact is assumed to be sticking followed by a sliding contact region which can be modeled by the Coulomb friction law. The model is useful predicting not only the cutting forces but the stress distributions on the rake face as well as the length of the sticking and sliding zones. The prediction of these regions will enable further predictions like temperature distribution in a more correct way, which is still under investigation. Also, the predictions of the model are compared with the experimental results, and overall a good agreement is observed. This agreement is expected since the friction coefficient between the tool and the workpiece material is calibrated by orthogonal tube cutting tests. Another comparison is done using the non-cutting friction tests in order to validate the sliding friction calculations, and again a good agreement is observed.
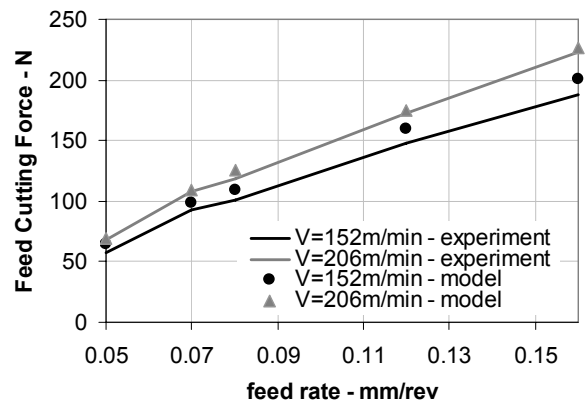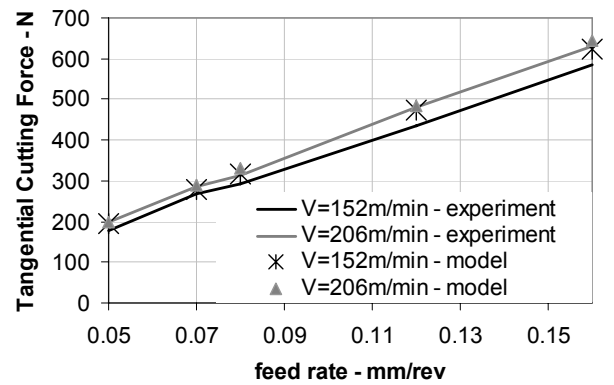

Figure 11: The comparison of the cutting forces predicted by the proposed process mode and the experimental results.

REFERENCES

[1] Merchant, E., 1945, Mechanics of the Metal Cutting Process I. Orthogonal Cutting and a Type 2 Chip, Journal of Applied Physics, 16/5, 267-275.

[2] Cumming, J. D., Kobayashi, S., and Thomsen, E. G., 1965, "A New Analysis of the Forces in Orthogonal Metal Cutting," ASME J. Eng. Ind., 87, pp. 480–486.

[3] Zorev, N. N., 1963, Inter-relationship between shear processes occurring along tool face and shear plane in metal cutting, International Research in Production Engineering, ASME, New York, 42-49.

[4] E.H. Lee and B.W. Shaffer, 1951, The Theory of plasticity applied to a problem of machining, Trans. ASME, J. Appl. Mech., 18, 405–413.

[5] M. C. Shaw, N.H. Cook, and I. Finnie, 1953, The Shear-Angle Relationship in Metal Cutting",. Transaction ASME, 75, 273-283.

[6] Palmer, W.B., Oxley, P.L.B., 1959, Mechanics of Orthogonal Machining, Proc. Instn. Mech. Engrs., 173/24, 623-638.

[7] Childs, T., 1980, Elastic Effects in Metal Cutting, Int. J. Mech. Sci., 22, 457-466.

[8] Armarego, E.J.A. and Whitfield, R.C. 1985, Computer based modeling of popular machining operations for force and power predictions. Annals of the CIRP, 34: 65-69.

[9] Budak, E., Altintas, Y. and Armarego, E.J.A., 1996, Prediction of milling force coefficients from orthogonal cutting data. Trans. ASME J. of Man. Sci. and Eng., 118, 216-224.

[10] Altintas, Y., 2000, Manufacturing Automation, Cambridge University Press.

[11] Lin, Z.C., Pan, W.C., 1995, Lo, S.P., A study of orthogonal cutting with tool flank wear ans sticking behavior on the chip-tool interface, J. Mat. Proc. Tech., 52, 524-538.

[12] Lo, S.P., Lin, Y., 2002, An investigation of sticking behavior on the chip-tool interface using thermo-elastic-plastic finite element method, J Mat. Proc. Tech., 121, 285-292.

[13] Yen, Y., Jain, A., Altan, T, 2004, A finite element analysis of orthogonal machining using different tool edge geometries, J. Mat. Proc. Tech., 146, 72-81.

[14] Umbrello, D., Saoubi, R., Outeiro, J.C., 2007, The influence of Johnson–Cook material constants on finite element simulation of machining of AISI 316L steel, Int. J. Machine Tools&Manufacture, 27, 462-470.

[15] Oxley, P.L.B., 1989, Mechanics of Machining, an Analytical Approach to Assessing Machinability, Ellis Horwood Limited, England.

[16] Fang, N, 2003, Slip-line modeling of machining with a rounded-edge tool – Part 1: new model and theory, J. Mechanics and Physics of Solids, 51, 715-742.

[17] Fang, N., Jawahir, I.S., 2001, A new methodologyfor determining the stress state of the plastic region in machining with restricted contact tools, Int. J. Mech. Sci., 43, 1747-1770.

[18] Maity, K.P., Das, N.S., A Class of slipline field solutions for metal machining with sticking-slipping zone including elastic contact, Mater Design, doi:10.1016/j.matdes.2006.07.014.

[19] Kudo, H., 1965, Some new slip-line solutions for two-dimensional steady-state machining, Int. J. Mech. Sci. 7, 43-55.

[20] Yellowley, I., 1987 A Simple Predictive Model of Orthogonal Metal Cutting, Int. J. Mach. Tools Manufact., 27/3, 357-365.

[21] Dudzinski, D., and Molinari, A., 1997, A Modelling Of Cutting For Viscoplastic Materials, Int. J. Mech. Sci, 39/4, 369-389.

[22] Moufki, A., Molinari, A., and Dudzinski, D., 1998, Modelling of Orthogonal Cutting with a Temperature Dependent Friction Law, J. Mech. Phys. Solids, Vol. 46/10, 2103-2138.

[23] Karpat, Y., Ozel, T., 2006, Predictive Analytical and thermal Modeling of Orthogonal Cutting Process – Part 1: Predictions of Tool Forces, Stresses, and Temperature Distributions, J. Manuf. Sci Eng., 128, 435-444.

[24] Bailey, J.A., 1975, Friction in metal machining-mechanical aspects, Wear, 31, 243-275.

[25] Philippon, S., Sutter, g., Molinari, A., 2004 An experimental study of friction at high sliding velocities, Wear, 257, 777-784.

[26] Tao, Z., Lovell, M.R., Yang, J.C., 2004, Evaluation of interfacial friction in material removal processes: the role of workpiece properties and contact geometry, Wear, 256, 664-670.

[27] Fang, N., 2005, Tool-chip friction in machining with a large negative rake angle tool, Wear, 258, 890-897.

[28] Childs, T.H.C., 2006, Friction modeling in metal cutting, Wear, 260, 310-318.

[29] Ozel, T., 2006, The influence of friction models on finite element simulations of machining, Int. J. Machine Tools&Manufacture, 46, 518-530.

[30] Kilic, D.S., Raman, S., 2006, Observations of the tool-chip boundary conditions in turning of aluminum alloys, Wear, doi:10.1016/j.wear.2006.08.019.

[31] Filice, L., Micari, F., Rizutti, S., and Umbrello, D., 2007, A critical analysis on the friction modeling in orthogonal machining, Int. J. Mach. Tools&Manufacture, 47, 709-714.

[32] Buryta, D., Sowerby, R., and Yellowley, I., 1994, Stress Distributions on the Rake Face During Orthogonal Machining, Int. J. Mach. Tools Manufact., 34/5, 721-739.

[33] Arsecularatne, J. A., 1997, On Tool-Chip Interface Stress Distributions, Ploughing Force and Size Effect in Machining, Int. J. Mach. Tools Manufact., 37/7, 885-899.

[34] Rabinowicz, E., 1995, Friction and Wear of Materials: Second Edition, Wiley-Interscience, New York, 102.

[35] Olsson, M.,Soderberg, S., Jacobson, S., Hogmark, S., 1989, Simulaton of cutting tool wear by a modified pin-on-disc test, Int. J. Mach. Tools Manufact., 29/3, 377-390.

[36] Kato, S., Yamaguchi, K., and Yamada, M., 1972, Stress Distribution at the Interface Between Tool and Chip in Machining, Journal of Eng. For Industry, 683-689.

[37] Barrow, G., Graham, T., Kurimoto, T., and Leong, F., 1982, Determination of Rake Face Stress Distribution in Orthogonal Machining, Int. J. Mach. Tool. Des. Res., Vol. 22, No. 1, 75-85.

[38] Maclain, B., Batzer, S.A., and Maldonado, G. I., 2002, A numeric investigation of the rake face stress distribution in orthogonal machining, J. Materials Proc. Tech., Vol. 123, 114-119.

[39] Altan, T., Oh, S., Gegel , H.L., 1983, Metal forming : fundamentals and applications, Metals Park, OH : American Society for Metals.